Proceedings of the
International Conference on Mechanical Engineering 2007
(ICME2007) 29- 31 December 2007, Dhaka, Bangladesh

ICME07-TH-21

NUMERICAL HEAT TRANSFER AND PRESSURE DISTRIBUTION ACROSS THE HEAT EXCHANGER IN A COOLING TOWER

M. M. A. Sarker[1*], M. R. Miah[22]

[1]Department of Mathematics, Bangladesh University of Engineering & Technology, Dhaka-1000, Bangladesh
* Corresponding author: E-mail: masarker@math.buet.ac.bd, Tel: +880-2-9665650/Ext. 7948
[2]Lecturer, Dept of Mathematics, Govt. Mujib College, Noakhali, Bangladesh

ABSTRACT

Heat transfer performance and pressure drop across the heat exchanger in a Hybrid Closed Circuit Cooling Tower (HCCCT) has been numerically studied. Flow characteristics have been analyzed using generalized non-orthogonal coordinate system. The problem related to pressure velocity coupling was handled using SIMPLE algorithm. In a HCCCT, process fluid remains completely isolated from the ambient air, so the quality of the process fluid is protected, and airborne contaminants are prevented from entering and fouling the system. Performance characteristics of the HCCCT were investigated using nominal operating condition. Pressure drop and cooling capacity were studied having air inlet located both at side wall and at the bottom end for different transverse pitches with variable velocities.

Keywords: Hybrid closed circuit cooling tower; Wet-bulb temperature; Cooling capacity.

1. INTRODUCTION

Cooling towers are a very important part of many chemical plants. A cooling tower rejects heat from water by evaporation. Evaporative cooling towers are relatively inexpensive and very dependable means of removing low-grade heat. Cooling towers are commonly used for providing cooled water for air-conditioning, manufacturing and electric power generation [1-2]. A closed circuit cooling tower which maintains an indirect contact between the fluid and the atmosphere that is do not allow the water to come into contact with any outside substance [3]. The water consumption rate of a cooling tower system is only about 5% of that of a once-through system, making it the least expensive system to operate with purchased water supplies. In addition, the amount of heated water discharged is very small, so the ecological effects like GWP (Global Warming Potential) and ODP (Ozone Depletion Potential) are greatly reduced. Cooling tower can be defined as a device whose main purpose is to cool water circulated through condensers or other heat-rejection equipment, by direct contact between the water and a stream of air [4-5].

Cooling towers are respectively called wet tower when evaporative cooling is used, dry tower when air blast cooling is utilized and wet-dry type which has the simultaneous characteristics of both dry and wet towers. Cooling effects in wet cooling towers are partially brought about by the evaporative condenser where a quota of the circulating water gets evaporated and partially by the sensible heat transfer. On the other hand, cooling effect is attained through convection and radiation heat transfer from any hot metal surface to an air stream moving across the surface and finally dissipating the heat into the atmosphere [6-8].

The hybrid closed circuit cooling tower (HCCCT) is a closed circuit cooling tower which is capable of working both in wet mode and in dry mode. HCCCT works well in dry mode during the mid-season and winter as soon as ambient temperature is below 12^{O}C, no plume and no freezing and lower noise level. HCCCT operates smoothly in wet mode during the summer while the ambient temperature is above 12^{O}C, water consumption by HCCCT is lower and the process water can be cooled down to 4^{O}C above the wet bulb temperature and can be packed in light and compact bundle with optimized circuitry [9].

In the HCCCT, water is sprayed in summer using squared form and wide angle spray nozzles from the top of the tower along with a counter-type of air flow in both summer and winter from the bottom part. In general, weather is warmer in summer, so both spray water and countertype air flow will be utilized to get the expected cooling effect. During the summer operation, no plume formation is expected due to the higher ambient temperature and higher dew-point temperature. In winter, only the cooled air from the bottom will be used to get the cooling effect and plume free state is predicted once more because the local winter ambient air contain lower moister.

The objective of this study is to investigate the heat transfer characteristics and pressure drop across the heat exchanger of a HCCCT having a rated capacity of 2RT (7 kW/h in SI unit).

2. DISCRETIZATION EQUATIONS

In the HCCCT, length is larger than the width, steady and stabilized sprayed water flow from the squared form and wide-angled spray nozzles can be considered to have the 2-dimensoional flow. It is required to combine all the basic equations and to put in a compact vector form to facilitate the computation. Using vector notation, the compressible Navier-Stokes (NS) equations in Cartesian coordinates can be written as

$$\frac{\partial Q}{\partial t}+\frac{\partial E}{\partial x}+\frac{\partial F}{\partial y}=\frac{\partial E_v}{\partial x}+\frac{\partial F_v}{\partial y}+S \qquad (1)$$

The physical domain of interest in a HCCCT is non-rectangular. To overcome the difficulties related to geometric complexity, a generalized coordinate system that maps the nonrectangular grid system from the physical space to the rectangular grid spacing in the computational space is applied. To define the relations between the physical and the computational spaces, the following general transformation is introduced:

$$\xi=\xi(x,y),\ \eta=\eta(x,y) \qquad (2)$$

Then for a two dimensional cell, we should have

$$\int_v \frac{\partial Q}{\partial t}dv+\int_{s_\xi}\vec{W}.\vec{n}_\xi\, ds_\xi+\int_{s_\eta}\vec{W}.\vec{n}_\eta ds_\eta=0 \qquad (3)$$

where the terms having subscripts ξ and η represent quantities along the stream wise and cross-stream wise directions respectively. The unit normal vectors are

$$\begin{aligned}\vec{n}_\xi&=\left(S_{\xi_x}\vec{i}+S_{\xi_y}\vec{j}\right)\Big/\left|\vec{S}_\xi\right|\\ \vec{n}_\eta&=\left(S_{\eta_x}\vec{i}+S_{\eta_y}\vec{j}\right)\Big/\left|\vec{S}_\eta\right|\end{aligned} \qquad (4)$$

The surface vectors $\vec{S}_\xi$, $\vec{S}_\eta$ can be given by

$$\vec{S}_\xi=S_{\xi_x}\hat{i}+S_{\xi_y}\hat{j}\ ,\quad \vec{S}_\eta=S_{\eta_x}\hat{i}+S_{\eta_y}\hat{j} \qquad (5)$$

S_ξ, S_η are the magnitudes of $\vec{S}_\xi$ and $\vec{S}_\eta$ respectively.

Utilizing Eqs. (2) & (3), Eq. (1) reduces to

$$\int_v \frac{\partial Q}{\partial t}dV+\int_{S_\xi}\left(E_\xi-E_{v_\xi}\right)dS_\xi+\int_{S_\eta}\left(F_\eta-F_{v_\eta}\right)dS_\eta=0 \qquad (6)$$

Control Volume Method is used for discretizing the partial differential equations and SIMPLE (Semi-Implicit Method for Pressure Linked Equations) algorithm of Patankar [10] has been utilized to handle the problem related to pressure-velocity coupling. The discretization equation for u is given by

$$a_P u_P=a_E u_E+a_W u_W+a_N u_N+a_S u_S+S_u \qquad (7)$$

where

$$a_E=D_e=\left\{\frac{\mu}{d\forall}\left(S_{\xi_x}{}^2+S_{\xi_y}{}^2\right)\right\}_e \qquad (8)$$

$$a_W=D_w=\left\{\frac{\mu}{d\forall}\left(S_{\xi_x}{}^2+S_{\xi_y}{}^2\right)\right\}_w \qquad (9)$$

$$a_N=D_n=\left\{\frac{\mu}{d\forall}\left(S_{\eta_x}{}^2+S_{\eta_y}{}^2\right)\right\}_n \qquad (10)$$

$$a_S=D_s=\left\{\frac{\mu}{d\forall}\left(S_{\eta_x}{}^2+S_{\eta_y}{}^2\right)\right\}_s \qquad (11)$$

$$a_P=a_E+a_W+a_N+a_S-S_p \qquad (12)$$

S_u is source term $S_u=S_{u'}+S_P u_P$, $S_{u'}=cp\times u(n)-dpdx$, $S_P=-cp=-Max[0,smp]$ and smp is the net outflow from the control volume (mass source). Here S_P represents all the terms those can not be approximated by values of u at the five points E, W, N, S and P. Here, upper case letters denote grid points and lower case letters denote the interface of the CV as shown in Fig. 1. $d\forall$ is the scalar area of a control volume. Similarly, discretization equation for v can be given by

$$a_P v_P=a_E v_E+a_W v_W+a_N v_N+a_S v_S+S_v \qquad (13)$$

Numerical details of this study can be found from Miah [11].

Discretized energy equation is

$$a_P T_P=a_E T_E+a_W T_W+a_N T_N+a_S T_S+S_t \qquad (14)$$

where

$$a_E=\left\{\frac{\mu}{prl\times d\forall}\left(S_{\xi_x}{}^2+S_{\xi_y}{}^2\right)\right\}_e \qquad (15)$$

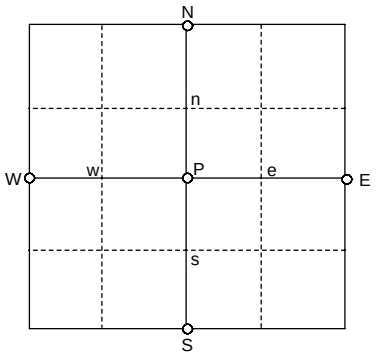

Fig 1: An internal control volume along with four neighbors

$$a_W = \left\{ \frac{\mu}{prl \times d\forall} \left(S_{\xi_x}{}^2 + S_{\xi_y}{}^2 \right) \right\}_w \quad (16)$$

$$a_N = \left\{ \frac{\mu}{prl \times d\forall} \left(S_{\eta_x}{}^2 + S_{\eta_y}{}^2 \right) \right\}_n \quad (17)$$

$$a_S = \left\{ \frac{\mu}{prl \times d\forall} \left(S_{\eta_x}{}^2 + S_{\eta_y}{}^2 \right) \right\}_s \quad (18)$$

$$a_P = a_E + a_W + a_N + a_S - S_p \quad (19)$$

$$S_{t'} = cp \times t(n) \quad (20)$$

Here *prl* is the laminar Prandtl number and *cp* has the identical representation as defined for *u* and *v*. Here, S_t is the source term given by $S_t = S_{t'} + S_P t_P$, *Sp* represents all the terms those can not be approximated by values of *t* at the five points E, W, N, S and P.

3. NUMERICAL SIMULATION OF THE HCCCT

Table 1 shows the geometrical parameters used in this simulation. Table 2 shows the basic operating condition in order for deriving the proper operating condition to select the best performance of the HCCCT.

4. RESULTS AND DISCUSSION FOR DRY MODE

4.1 The Flow Characteristics inside HCCCT

The internal flow behavior is being checked in this section starting with the velocity vectors. The inlet is located at the bottom end of the tower and three passes are used for forcing the air into the tower. Fig. 2 gives the velocity vector's pattern where the right one gives a magnified view of the predicted air flow through the heat exchanger. The velocity of the air was found to be higher

Table 1: Geometric parameters of HCCCT

Length of the heat exchanger	[m]	0.7
Width of the heat exchanger	[m]	0.65
Height of the heat exchanger	[m]	1.12
Number of coils at heat excanger	[-]	16×7

Table 2: Simulation condition

Process fluid	Mass flow rate	[kg/h]	1000 ~ 1700
	Inlet temperature	[^{O}C]	37
Spray water	Mass flow rate	[kg/h]	1600 ~ 2500
Air	Velocity	[m/s]	1.5 ~4.0
	Inlet WBT	[^{O}C]	15 ~ 32

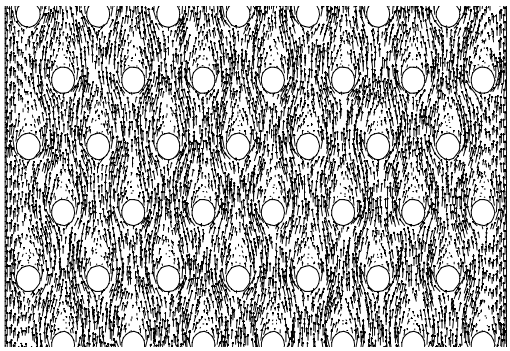

Fig. 2 Velocity vector inside HCCCT

around the air inlet and several turbulences have been formed over there. The predicted air flow at the bottom part of the tower is seen to be a bit non uniform but as the flow approaches the heat exchanger, it gets more and more uniform and right at coil bank, it could be claimed that the air flow is uniform.

4.2 Temperature Distribution by Air Velocity

In dry mode, only air is used from the bottom to cool the coils and the velocity of the air plays an important role both for the pressure drop and cooling capacity. We checked the influence of the air velocity for 4 different cases namely for an inlet velocity of 1.5, 2, 2.75 and 3 m/s. The temperature of the cooling water is seen to decrease with the increase of the air velocity. In a constant air temperature of 15^{O}C and a constant cooling water temperature of 37^{O}C were used for all the cases with a cooling water mass flow rate of 1600 kg/h. A comparative temperature distribution along the coil height is given in Fig. 3. The row number 16 in Fig. 3 implies the highest elevation of the heat exchanger and row 1 means the lowest part of the coil bank. The temperature of the cooling water is seen to decrease almost linearly for the increase of the air velocity and for the highest air velocity of 3 m/s, the temperature drop is the highest which is about 1.48^{O}C and at a simulation condition of 2.75 m/s, the temperature drop is 1.37 ^{O}C. So, the cooling capacity of HCCCT is about 2192 kcal/h.

4.3 Temperature Drop by Cooling Water Inlet Temperature

The cooling water inlet temperature can bring notable

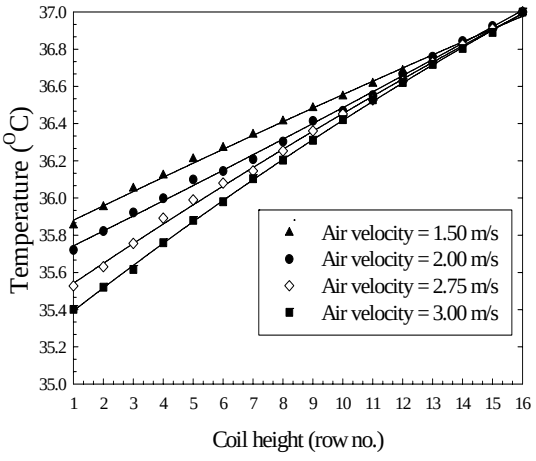

Fig. 3 Temperature distribution w.r.t. air inlet velocity

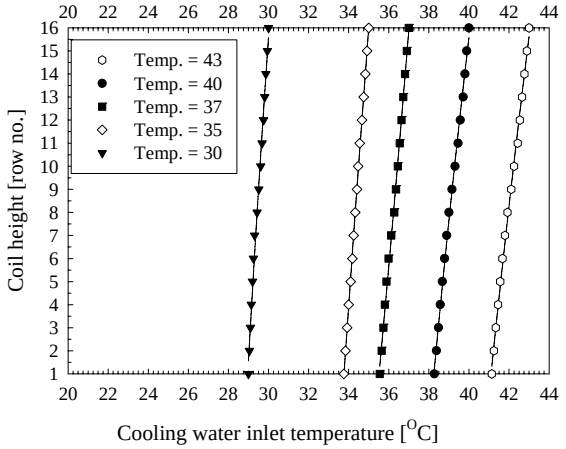

Fig. 4 Temperature drop by cooling water inlet temperature.

difference in the cooling capacity. The influences of the cooling water inlet temperature for 5 different cases of 30, 35, 37, 40 and 43^{O}C have been investigated. This time, a constant inlet air temperature of 15^{O}C and a constant cooling water mass flow rate of 1600 kg/h were used. The temperature is seen to decrease more rapidly for the cooling water having higher inlet temperature. A comparative temperature distribution along the coil height is shown in Fig. 4. The temperature is seen to decrease almost linearly. The temperature drop, which is calculated subtracting the temperature of the lowest coil from that of the top most coil, is seen to be higher for the cooling water having temperature of 43^{O}C. Although the higher cooling effect can be obtained having high inlet cooling water temperature but the outlet cooling water temperature is also high for higher inlet cooling water temperature which is undesirable. At the simulation condition of 37^{O}C, the temperature drop is 1.35^{O}C. Therefore, the cooling capacity is about 2160 kcal/h.

4.4 Temperature Drop by Air Inlet Temperature

The air inlet temperature can influence the cooling capacity. The impact is especially noteworthy for the dry mode operation of the HCCCT. The influences of the air inlet temperature for 4 different cases of 5, 10, 12, and 15^{O}C have been studied. A comparative temperature

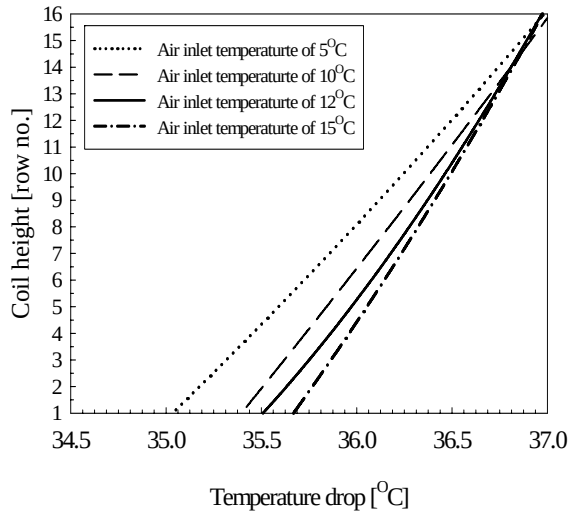

Fig. 5 Temperature distribution w.r.t. air inlet temperature

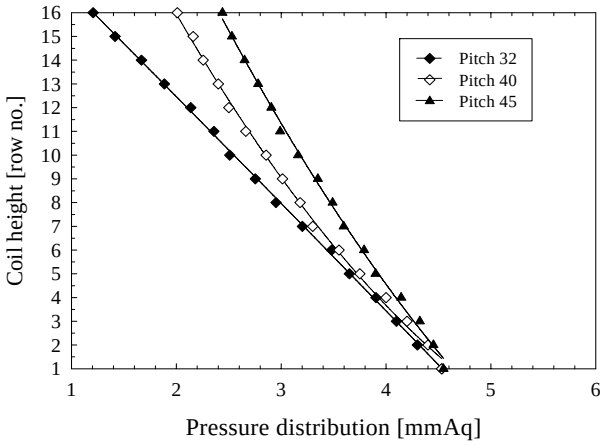

Fig. 6 Pressure distribution with respect to the coil pitch

distribution along the coil height is given in Fig. 5. The temperature is seen to decrease almost linearly along the coil height. The temperature drop is seen to be higher for the lower air inlet temperature. At the condition of 15^{O}C, the temperature drop is 1.37^{O}C. The cooling capacity is about 2192 kcal/h.

4.5 Pressure Having Air Inlet at the Side Wall

The coil pitch plays a very important role for raising the heat transfer brought about by the passing air and water flow through heat exchanger in a HCCCT. Too small spacing between the coils can reduce the velocity of the air and water and thereby the heat transfer efficiency can be lower as well. Especially, at the air side, more pressure drop causes even more power requirement by the fan. Pressure drops decreased with the increase of the coil's transverse pitches as expected. For 32, 40, and 45 mm pitches, the air velocities at the inlet were maintained to remain constant at 3.1 m/s. From Fig. 6, it is clear that the coils having higher pitch has lower pressure drop and vice versa and that all three cases has similar pressure at the lowest coil due to the constant inlet air flow rate. Coil having a transverse pitch of 45 mm produced lower pressure drop which was about 2.05 mmAq. Increasing the pitches are not a wise idea only for the sake of reducing the pressure drop because minimizing the pressure drop and the flow rate of the fluids can minimize the operating cost but it can maximize the size of the heat exchanger and thus the initial cost.

5. RESULTS AND DISCUSSION FOR WET MODE

5.1 Temperature Range by WBT

The temperature range of the cooling water with respect to wet bulb temperature having a variable cooling water flow rate is shown in Fig. 7. The heat exchanger's common feature/trend that the temperature range decreases with both the increases of the WBT and the cooling water flow rate and vice versa as can be seen from this figure as well. In the standard condition, the temperature range found is around 4^{0}C at WBT 27^{0}C.

5.2 Cooling Capacity in Wet Mode by WBT

The cooling capacity in wet mode operation of the HCCCT w.r.t. WBT having different cooling water flow

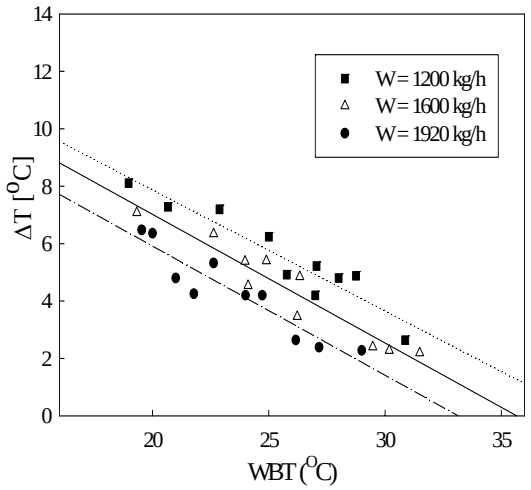

Fig. 7 The temperature range of the cooling water by WBT

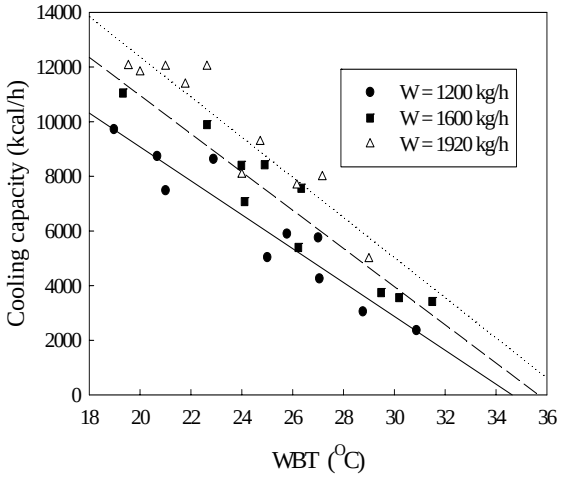

Fig. 8 The cooling capacity in wet mode operation against WBT

rate has been shown in Fig 8. It can be seen that the cooling capacity increases with the increase of the cooling water flow rate but decreases with the increase of the WBT followed by the decrease of the cooling water flow rate. At the design condition, the capacity at a WBT of 27^0C was about 6400 kcal/h, which is 18% lower than the rated one. The assumed cooling water mass flow rate of 1600 kg/h could be a reason.

5.3 Pressure Drop with Variable Airflow Rate

The pressure drop inside the heat exchanger of the HCCCT with respect to WBT having variable airflow rate has been shown in Fig. 9. Pressure drop is seen to increase with the increase of both the airflow rate and the WBT. At an airflow of 2.75 m/s and at WBT = 27^OC, static pressure drop was to be 2.2 mmAq and the about 3.3 mmAq for the air velocity of 3.1 m/s.

6. CONCLUSION

Numerical simulation has been performed for the HCCCT having a rated capacity of 2RT. In dry mode, at a simulation condition that is at an air velocity of 2.75 m/s,

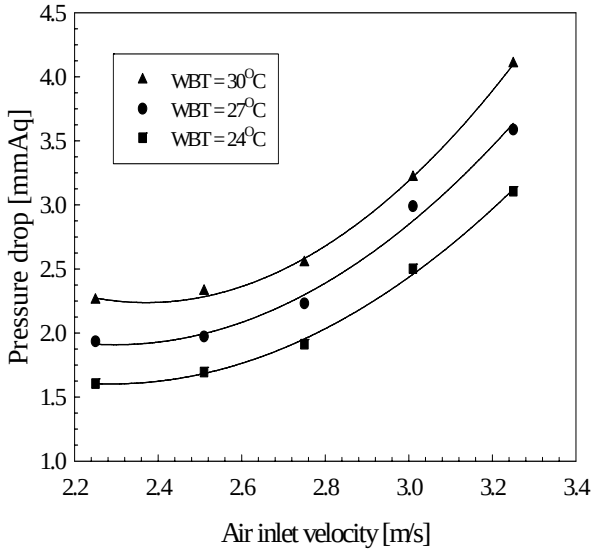

Fig. 9 Pressure drop in a HCCCT in wet mode

the temperature drop was 1.37 ^{O}C. Therefore, the cooling capacity of the HCCCT was about 2192 kcal/h. The temperature drop with respect to cooling water inlet temperature was 1.35^{O}C and hence the cooling capacity was about 2160 kcal/h. The temperature drop with respect to air inlet temperature was 1.37^{O}C and the capacity was about 2192 kcal/h.

In wet mode operation, the temperature range of the cooling water found was around 4^0C at WBT 27^0C and hence at the nominal simulating condition, the cooling capacity was about 6400 kcal/h, which is 18% lower than the rated one.

When the air inlet was located at the side wall of the HCCCT and having a transverse pitch of 45 mm produced lowest pressure drop in both modes. In dry mode, the pressure drop at an air velocity of 3.1 m/s was about 2.05 mmAq and in wet mode, the pressure drop was 2.2 mmAq and 3.3 mmAq for the air velocity of 2.75 m/s and 3.1 m/s respectively.

The results obtained from the numerical study of the performance characteristics of HCCCT is expected to serve as basic data that could be referred for the optimum design of heat exchanger in a hybrid type closed circuit cooling tower having a rated capacity of 2RT.

7. REFERENCES

1. Bergstrom, D.J; Derksen, D; Rezkallah, K.S, 1993, “Numerical study of wind flow over a cooling tower”, Journal of wind engineering and industrial aerodynamics, Vol. 46: 47, pp.657-664.
2. Hawlader, M. N. A; Liu, B. M, 2002, “Numerical study of the thermal-hydraulic performance of evaporative natural draft cooling towers”, Applied Thermal Engineering, Vol. 22:1, pp. 41-59.
3. Dreyer, A. A; Erens, P. J, 1996, “Modeling of cooling tower splash pack”, International Journal of Heat and Mass Transfer, Vol. 39:1, pp. 109 -123.
4. Jameel-Ur-Rehman Khan, Yaqub, M; Syed, M. Z, 2003, “Performance characteristics of counter flow wet cooling towers”, Energy Conversion and

Management, Vol. 44:13, pp. 2073-2091.
5. Jaber, H; and Webb, R.L, 1989, “Design of cooling towers by the effectiveness-NTU method”. ASME J. Heat Transfer, Vol. 111:4, pp. 837–843.
6. Gan, G; Riffat, S.B; Shao, L, Doherty, P, 2001, “Application of CFD to closed-wet cooling towers”, Applied Thermal Engineering, Vol. 21:1, pp. 79-92.
7. Ibrahim, G.A; Nabhan, M.B.W; Anabtawi, M.Z, 1995, “An investigation into a falling film type-cooling tower”, Int. J. Refrig, Vol. 18, pp. 557–564.
8. Baker, D. R; and Shryock, H. A, 1961, “A comprehensive approach to the analysis of cooling tower performance”, J. of Heat Transfer, Vol. 83, No. 3, pp. 339-350.
9. Al-Nimr, M. A, 1998, “Dynamic thermal behavior of cooling tower”, Energy conversion and management, Vol. 39:7, pp. 631-636.
10. Suhas V. Patankar, 1980, “Numerical heat transfer and fluid flow”, Hemisphere Pub. Corp., McGraw-Hill.
11. Miah, M. R, 2007, “Numerical Study of the Cooling Capacity and Pressure Drop in a Hybrid Closed Circuit Cooling Tower”, M. Phil thesis, Dept. of Math, BUET, Dhaka-1000, Bangladesh